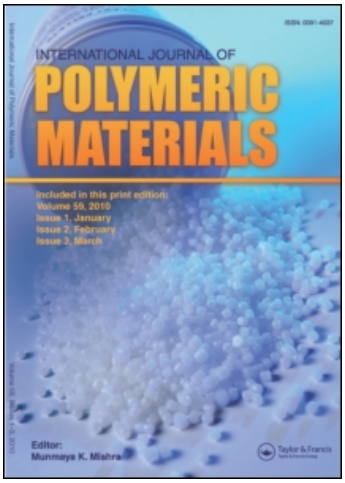

International Journal of Polymeric Materials
Publication details, including instructions for authors and subscription information:
http://www.informaworld.com/smpp/title~content=t713647664

Towards a non-CVD process for high-performance C-C composites: Part II

D. C. Prevorsek[a]; H. L. Li[a]; R. K. Sharma[a]; H. B. Chin[a]
[a] AlliedSignal Inc., Morristown, New Jersey, USA

Online publication date: 27 October 2010

To cite this Article Prevorsek, D. C. , Li, H. L. , Sharma, R. K. and Chin, H. B.(2002) 'Towards a non-CVD process for high-performance C-C composites: Part II', International Journal of Polymeric Materials, 51: 5, 451 — 473
To link to this Article: DOI: 10.1080/00914030214767
URL: http://dx.doi.org/10.1080/00914030214767

International Journal of Polymeric Materials, 51:451–473, 2002

0091-4037/02 $12.00 + .00
DOI: 10.1080/00914030290046039

TOWARDS A NON-CVD PROCESS FOR HIGH-PERFORMANCE C–C COMPOSITES: PART II

D. C. Prevorsek, H. L. Li, R. K. Sharma, and H. B. Chin
AlliedSignal Inc. Morristown New Jersey, USA

Part I of this study covered the matrix and pocessibility studies to establish the feasibility of a non-CVD process for manufacturing high performance C–C composites. Part II of this study covers the overview of Carbonization and Graphitizations investigations that ultimately led to a satisfactory product in processing times that were more than an order of magnitude shorter than those of typical CVD processes.

Keywords: carbon–carbon composites, non-CVD process, carbonization, graphitization, matrix structure, mechanical properties, friction wear

INTRODUCTION

The performance of C–C composites is strongly affected by the starting materials, processing techniques and their final structure. In part I we reviewed our matrix and processibility investigations [1–10]. Here, we present the results of our carbonization and graphitization research, and product optimization.

Carbon fiber preforms used in high preformance carbon composites consist of highly porous fiber networks. A densification step is, therefore, needed to convert these preforms into useful carbon–carbon (C/C) composites.

Two main techniques are commonly used to densify the composites by impregnation: Chemical Vapor Deposition (CVD) and the Liquid Impregnation Process (LIP) [11, 12]. Due to the economical and technical advantages, the LIP has become more popular. LIP process involves the impregnation of the preform structure with pitch or other organic resins followed by carbonization/graphitization. In order to achieve the desired properties of the composite, many steps of impregnation/carbonization/graphitization are required.

Received 20 July 1999.
Address correspondence to D. C. Prevorsek, P.O. Box 677, Hood River OR 97031, USA.

Amorphous or glassy pitch can be converted to a carbon, or a coke, that is usually graphitizable when it is heated in inert atmosphere. It can be transformed to graphite when it is further heated to temperatures in excess of 2500°C. The ease with which carbons can be converted to graphite depends on the nature of carbon precursor [11–14].

Several techniques have been reported [12, 15–20] to provide qualitative and quantitative information regarding the structure of carbon, such as crystalline size and orientation, stack height and width, the sharp and size of pores and defect, morphology of glassy and graphitic carbon phases, and the presence of three-dimensional order. These techniques include wide- and small-angle X-ray diffraction, electron diffraction, transmission, scanning and surface replica electron microscopy, and optical microscopy.

The structure of the graphitzable carbon is usually described in terms of "turbostratic" layer packets or "crystallites" of height L_c and diameter or width L_a which are determined from the broadening of the [001] and [hk0] X-ray diffraction lines respectively. In the graphitizable carbons, L_c and L_a increase continuously with increasing heat treatment temperature (HTT). When graphitization takes place at temperatures exceeding of 2000°C, the width L_a becomes very large which is characterized by appearance of [hkl] reflections and a marked decrease in the interlayer spacing (d_{002}) to a value of 0.335 nm which is a characteristic of crystalline graphite. Other properties such as electronic and magnetic are also abruptly changed when graphitization occurs.

The role of the graphitization process variables on the performance of the carbon–carbon composites is very complex and not well-understood because the process requires very high processing temperature (1500–3000°C) and the matrix is gradually transformed from an amorphous glassy carbon structure into highly ordered graphitic structure during the heat treatment [20–30].

Furthermore, the graphitic structure in the matrix may not be uniform and it depends on process variables. For instance, thermally induced tensile or compressive stresses acting at the fiber-matrix interface may cause formation of localized stress graphitization [31].

Applications of hydrostatic pressure during the heat treatment have a dramatic accelerating effect on the graphitization of both soft (mesophase pitch) or hard (glassy) carbon [31–33]. Other than this, very little has been reported on the effect of pressure on the structural changes of the C/C composites induced by the flow of the C/C composites during densification at extraordinarily high processing temperature (1500–3000°C). To develop a one-step C/C composite process we studied the effect of processing variables (pressure, time, and temperature) on the structural changes induced by the flow of the C/C composite during densification.

EXPERIMENTAL

Carbonization/Graphitization Equipment

Three different furnaces were used in this study for the study of high temperature carbonization/graphitization. The first type is the induction heating hot-press, and the second one is a hot isostatic press (HIP) furnace, and the third type is conventional high temperature hot press (HP) furnace.

Induction Heating Hot-Press

The induction heating furnace equipped with a plunger was made by GCA/Vacuum Industries (PA). The induction heater was designed by Inductotherm, Inc. with 22 kw output. This furnace can be used for carbonization/graphitization process and its capabilities are:

1. Environmental chamber:
   a. Dimensions: 24″ dia. × 18″ depth
   b. Equipped with vacuum or inert gas pressurized facilities
2. Hydraulic press tonnage: 50 tons max.
3. Power input: 22 kW max.
4. Sample size: 0.5″ to 5″ dia. max; 5″ height max.
5. Maximum Temperature: 2,000°C max.

Hot Isostatic Press

The hot isostatic press (HIP) was made by IPS, Inc. (Ohio). The specification of the capacity of the HIP furnace are:

1. Atmosphere: Inert
2. Max Pressure: 1.5 ksi(Isotatic)
3. Max Temp: 2100°C
4. Maximum Sample Size: (in the Hot Zone) 4″ diameter, 7″ height

Conventional Hot Press

The conventional high temeprature hot-press (HP) was made by Centorr, NH (now consolidated with Abar Ipsen, IL). The specification of the capacity of the HP furnace are:

1. Atmosphere: Argon
2. Max Loading: 1000 lbf
3. Max Pressure: 3 – 5 ksi (depending on the diameter of the part)
4. Max Temp: 2200°C
5. Maximum Sample Size: Depending on the required pressure

The hot press is equipped with a LVDT transducer to register the dimensional change behavior in the axial direction during the densification process. The data were recorded every 50 seconds and stored in a computer.

Carbonization Experiments

As discussed earlier, the equipment used for compaction/carbonization was manufactured by Vacuum Industries. As seen in Figure 1 it is comprised of

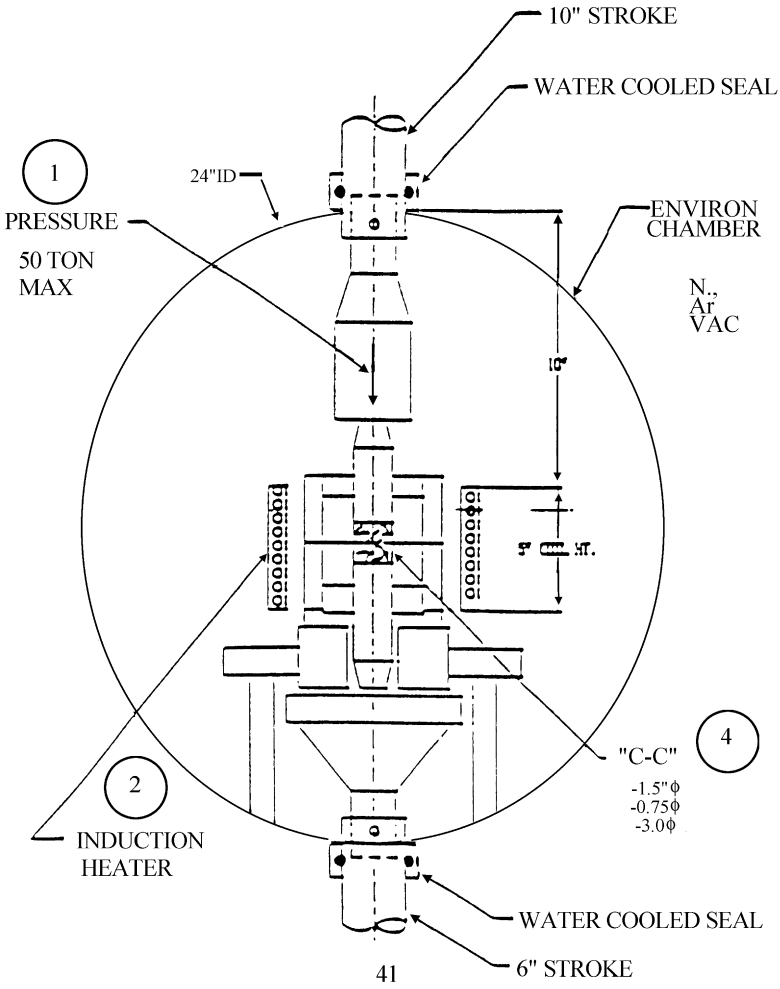

FIGURE 1 Schematic of the 3-component unit of the induction press.

three main components:

1. *Hydraulic unit*: It consists of dual action hydraulic cylinders which can push the preform either up or down, or hold in neutral position under a max. pressure of 50 tons.
2. *Induction heater*: The heater was designed by Inductotherm, Inc. with 22 kw output. The induction coils, made from 0.75″ dia. copper tubing, has approx. 12″ O.D. × 10.5″ I.D. × 6 turns, which is internally water cooled.
3. *Environmental chamber*: The environmental chamber, measured 24″ diameter × 18″ depth, was designed to hold high vacuum and inert gas to prevent oxidation during carbonization.

Figure 2 shows the equipment design of the plunger and mold arrangement for compaction/carbonization (or molding preforms to form

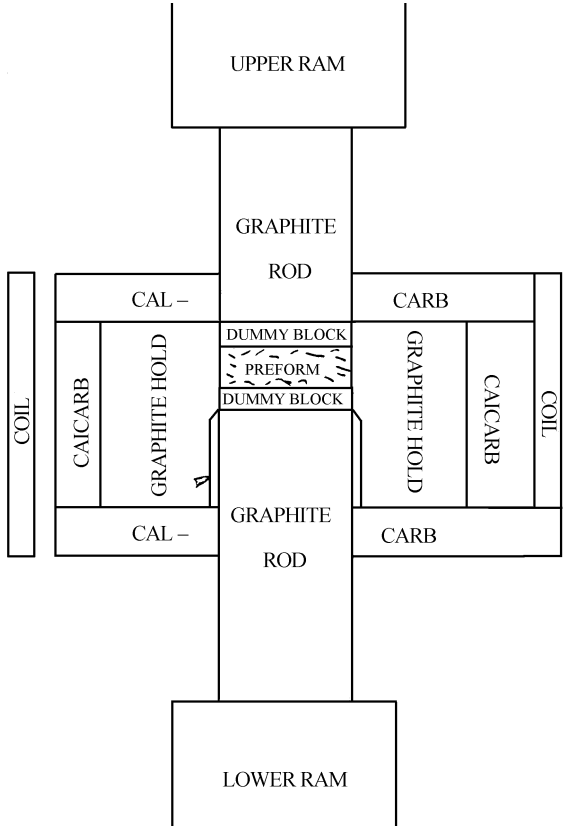

FIGURE 2 The plunger and mold arrangement.

C–C composites) in single step process. The preform is sandwiches between two dummy blocks.

The cylindrical mold, 3″ I.D. × 8″ O.D. × 6″ L, is machined from Poco high strength graphite and insulated with Calcarb tube, a rigid graphite foam, graphite felt and Zircon felt. All of these insulating materials are also susceptible to induction heating which makes it possible to heat the C–C samples up to a maximum temp. of 2,000°C.

During heating, the preform was compressed by two graphite rods of 2.995″ diameter under hydraulic pressure. Compaction/carbonization was carried out under heat and pressure.

With this arrangement, we are able to process different types of preforms (such as in the form of RTM stitched carbon felt and chopped impregnated or pultraded carbon fiber preforms) free of defects such as cracks in the one-step non-CVD process of compaction/carbonization. In the following, we are discussing the process of compaction/carbonization of RTM carbon felt and the pultruded chopped carbon fibers.

Compaction/Carbonization of RTM Carbon Felt Experiments

3″ diameter × 0.5″ thick C/C disc (sample #A84T) – The stitched carbon felt, was resin impregnated with pitch resin using resin transfer molding technique. The preform contained about 40% by weight of carbon felt and 60% of meso pitch as resin. The preform measured 3″ diameter × 1.2″ thick with an apparent density of 1.2 gm/cc was heated in a vacuum oven flushed with argon inert gas under temperature 450°C for 3 hours to remove volatile and also increase the viscosity of the resin to prevent leakage from the mold during the pressure cycle.

The treated preform was placed inside the cylindrical mold of 3″ ID and heated from room temperature to 1000°C under a pressure of 7 ksi. The heating rate was approximately 15°C/min. The location of the partially carbonized preform within the mold is shown in Figure 2. As soon as the temperature exceeded 1000°C, the carbonized preform was pushed downward to a section with an enlarged diameter of 3.045″, qualitatively shown in Figure 2, to reduce the radial pressure due to thermal coefficient of expansion. Otherwise, severe cracks were observed. The sample was further heated to 1400°C and kept for 5.5 hours. Cooling down was followed under 7 ksi. The total cycle time was 8.5 hours. The C/C sample has a density of 1.6 gm/CC.

Compaction/Carbonization of Chopped Carbon Fibers

This example illustrates compaction/carbonization of pultruded and chopped carbon fibers into 0.75″ diameter C/C composite disc. The carbon

fibers, PAN based AMOCO T-300, 3K, unsized, were pultruded with Ashland-A80 petroleum pitch as matrix resin. The pultruded fibers were then chopped into approx. 0.5″ in length and heat treated at 440°C for one hour to increase the viscosity level to prevent leakage from the mold during compaction/carbonization. The weight ratio between carbon fiber to resin was 12% to 88%. The 0.5″ chopped pultruded fibers, weighed about 4.4 grams, were charged into a graphite mold of 0.75″ diameter which was heated from 23°C to 525°C under 1.0 ksi pressure and then from 525°C to 1000°C at a heating rate of 30°C/min under a pressure of 12.9 ksi. The compacted chopped fibers, or preform, was held at 1,000°C for half an hour before cooling cycle started. The carbonized sample with a diameter of 0.75″ and height of 0.396″ which corresponding to a density of 1.52 gm/cc.

Multiple samples can be made under the same arrangemment and conditions. In one experiment, three carbonized samples were stacked into the same mold and graphitized to 2,000°C for about 4 hours. The stacked graphitized samples have the similar density characteristics as the single sample.

Graphitization Experiments

A typical procedure and cycle in the graphitization by the conventional hot-press is illustrated in Figure 3. Similar to the induction heating hot-press, the process parameters such as pressure, time, and the temperature can be changed depending on the product specification of the structure/properties of the C/C composite.

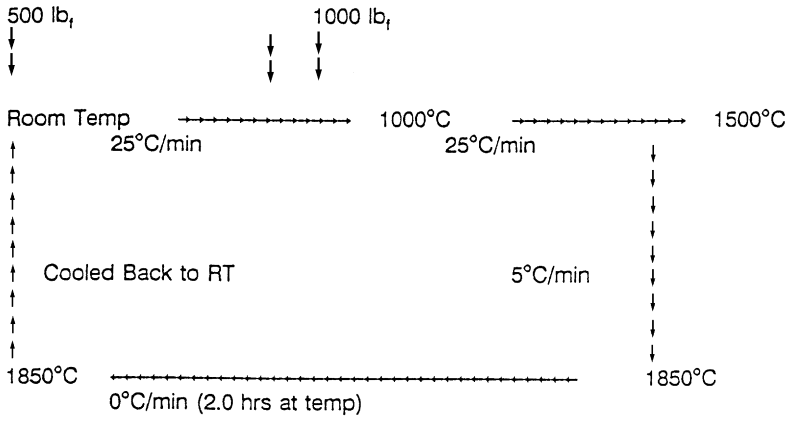

FIGURE 3 Graphitization conditions (argon atmosphere).

Characterizations

The following properties were evaluated:

1. density,
2. porosity,
3. carbon structures,
4. compressive strength

Density Measurement

Both pycnometry and gravimetry were used to measure density of the C/C composite at room temperature.

X-ray Diffraction Measurement

The wide angle X-ray diffraction was used to determine the structure of the C/C composite. In addition to the measurement of the d_{002} and d_{100} spacing, the dimensions of the "turbostratic" layer packets or "crystallites" of height L_c and diameter or width L_a are also determined from the broadening of the [00l] and [hk0] X-ray diffraction lines respectively.

Porosity Measurement

Both mercury porosimetry and density measurement were used to determine the porosity of the C/C composite. In the mercury porosimetry, we assumed the critical contact angle is 140°C and surface tension of mercury is 485.0 dynes/cm.

Compressive Strength

The compressive strength of the samples was evaluated in a press equipped with a force gauge. The compressive strength is determined from the ultimate force required to destroy the sample divided by its surface area.

RESULTS AND DISCUSSION

Carbonization Process

The carbon structure in the one-step "carbonized" C/C composites (HTT < 1000°C) is still amorphous. As is seen from Table 1, the carbon structure found in the carbonized composites derived from two different pitch matrices is very similar, but its dimensions are smaller than those found in the commercial aircraft brakes.

Density Measurement

The density of the graphitizable pitch resin increases continuously with increasing heat treatment temperature (HTT). The density of the untreated pitch is about 1.24 gm/cc. The density of the same material increases to

TABLE 1 Effect of mode of pressing on densification (1000°C, 4 hours, 4 kpsi)

Spacing, nm		*Graphite crystal*	*CVD control*	*Two non-CVD composites*	
	$d_{(002)}$	0.335	0.342	–	–
1. $d_{(hkl)}$	$d_{(100)}$	0.213	0.212	0.209	0.208
2. $L_{c,\ (002)}$		Large	11.8	1.8	1.8
3. $L_{a,\ (100)}$		Large	6.3	2.3	2.1

1.60 gm/cc after it was treated at a temperature of 1000°C and to 1.70 gm/cc after it was treated at 2050°C.

The density of the one step (non-CVD) C/C composite can be made to match or exceed the density of the CVD commercial products. We have studied the effect of the parameters (such as mode of press, type of preform, time, temperature, and pressure) which affect the densification process and which ultimately affect the final density of the C/C composites. We report the results in the following sections on densification.

Porosity Measurement

Both mercury porosimetry and density measurement were used to determine the porosity of the C/C composite. For a one step (Non-CVD) C/C composite whose density is 1.555, we calculated its porosity is about 20.6%. The porosity of the same sample was evalated by the mercury porosimetry. With the assumption that the critical contact angle is 140° and surface tension of mercury is 485.0 dynes/cm, we found that the % pore volume is 19.5. The pore volume is about 0.122 cc/gm, the average pore area is about 10.3 m^2/gm, and the average pore diameter is about 0.047 micron. Therefore, the porosity determined from the density calculation is fairly accurate. Also, the dominating pore morphology in this type of C/C composite was found to be open-pore structure from the density and the porosimetry measurement.

Processing Parameters Affecting the Densification Process

Effect of Mode of Press

The effect of the isostatic mode and hot-press mode of pressing on density is illustrated in Table 2. All the samples were fabricated at 1850°C and 1.4 kpsi for 2.0 hours. The hot-press process provides denser composites than isostatic process. Therefore, we have decided to use the hot-press process in the research of the development of the one-step (non-CVD) C/C composite.

TABLE 2 Effect of mode of pressing on densification (1850°C, 2 hours)

Starting carbonized composite		*Density, gm/cc* / *Porosity, %*	1.55 *gm/cc* / 21.8%
Graphitized Composite	Hot-press	Density, gm/cc	1.62 gm/cc
		Porosity, %	12.9%
	Isotatic	Density, gm/cc	1.44 gm/cc
		Porosity, %	34.1%

Effect of Type of Molding Compound

The effect of the type of molding compound on density is given in Table 2. All the samples were fabricated at 1850°C and 5.0 kpsi for 2.0 hours by hot-pressing. As seen in Table 3, both dry-mixed and melt-impregnated molding compounds can be densified by hot-press process.

Effect of Pressure on Densification

The effect of pressure during isothermal densification by hot-pressing at 2000°C for 4 hours under Argon was given in Table 4.

As we can seen from Table 4, the pressure plays a critical role on density, porosity, and volume shrinkage characteristics of the carbon–carbon

TABLE 3 Effect of type of molding compound (hot press, 1850°C, 5 ksi)

Type of molding compound		*Dry-mixed*	*Melt-impregnated*
Starting carbonized composite	Density, gm/cc	1.55 gm/cc	1.44 gm/cc
	Porosity, %	21.2%	34.1%
Graphitized composite	Density, gm/cc	1.62 gm/cc	1.64 gm/cc
	Porosity, %	12.9%	10.6%
Weight loss (wt%)		9.4	7.0
Shrinkage, %	Thickness	11.7	17.9
	Volume	15.1	18.0

TABLE 4 Effect of pressure

	Before	*After*			
Graphitization→ Pressure↓	*Density, gm/cc*	*Density, g/cc*	*Porosity, %*	*Weight, loss, %*	*Volume shrinkage, %*
2.26 kpsi	1.50	1.63	11.8	4.65	14.0
1.13 kpsi	1.50	1.57	18.8	3.27	12.1
0.45 kpsi	1.52	1.55	21.2	3.28	6.91

composites. As expected, the volume shrinkage is in good argeement with porosity, which is affected by the magnitude of pressure applied during the densification process.

The effect of pressure on isothermal densification of the carbon–carbon composites in a hot-press under Argon is illustrated in Figure 4. Figure 4 gives a plot of percentage of density increase *versus* densification pressure. The percentage of density increase (ρ_1) is calculated from the equation:

$$\rho_1 = [(\rho_G - \rho_c)/\rho_c] \times 100\%$$

where ρ_G is the density of graphitized composites and ρ_c is the density of carbonized composite.

Several points are worth noting in Figure 4. (1) ρ_1 is negative (~5.1%) at zero densification pressure. (2) ρ_1 becomes positive when only very small amount of pressure (~200 psi) is applied in the graphitzation process. (3) ρ_1 increases rapidly with increasing pressure and (4) once the pressure reaches to about 7 kpsi, rate of ρ_1 increase slows down and (5) at 10 kpsi, it levels

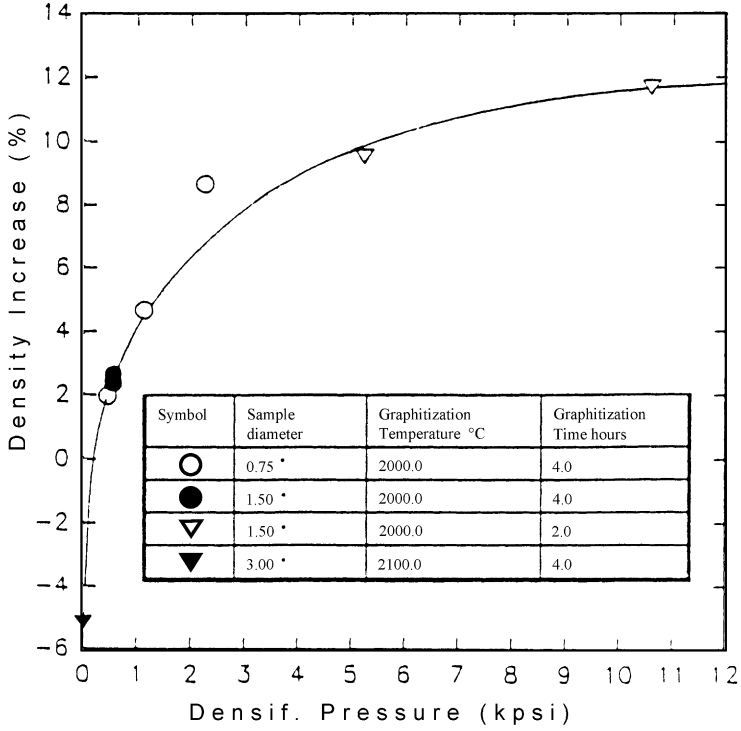

FIGURE 4 % Density increase *vs.* densification pressure.

off at a constant value about 12%. This finding is important in the processing of the one-step C/C composites by hot press. The optimum processing pressure within the conditions used in these experiments is about 5 to 7 kpsi.

Effect of Time on Densification

The effect of time on densification at 2000°C by the hot pressing was studied. The hot press is equipped with a LVDT transducer to register the dimensional change behavior in the axial direction during the densification process. The data were recorded every 50 seconds and stored in a computer. This dimensional change of the materials is calculated after subtraction of the total dimensional change in the axial direction from the calibrated dimensional changes in the axial direction of the thermal expansion and the deflection of the press due to the axial loads.

As seen from Figure 5 for the isothermal densification experiments conducted at 2000°C, the dimensional change of the C/C composites depends strongly on the time of densification and the level of pressure. We should point out that the dimensional change characteristics in the radial direction are equally important to determine the performance of the C/C composites.

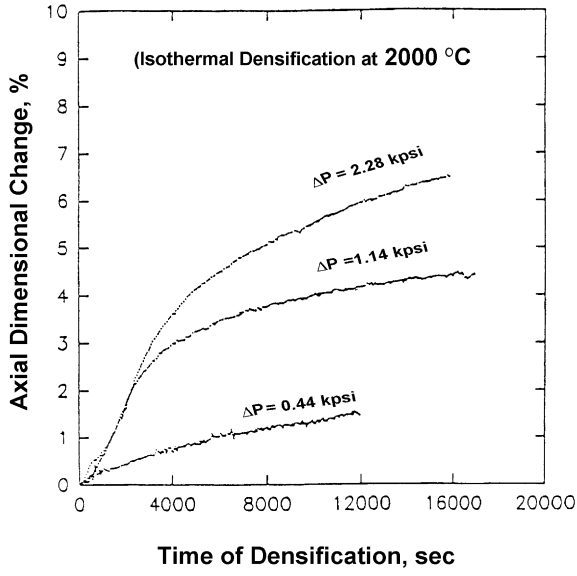

FIGURE 5 Axial dimensional changes *vs.* time of densification.

Processing Parameters Affecting the Carbon Structure

Figure 6 gives the wide-angle diffraction patterns of a commercial CVD control and of a one step non-CVD C/C composite. As seen from this Figure, the carbon structure of both composites are very similar.

Figure 7 presenting the d_{100} spacing of the commercial product and of two one step C/C composite samples shows, however, that the structure of the carbonized C/C sample has not yet been developed to the level of the graphitized one step C/C composite and that of the commercial product.

Effect of Time

The effect of time of graphitzation on the carbon structure of the C/C composite is given in Table 5. The pitch matrix for these sample was RS–A 80. All the samples were fabricated at 1850°C and 5.0 kpsi by hot-pressing. As indicated from Table 5, the dimensions of carbon structure grow with time. The structure grown for 4 hours is closest to that found in the commercial product.

Effect of Temperature

The effect of graphitzation temperature on the carbon structure of the C/C composite is given in Table 6. The pitch matrix for these sample was

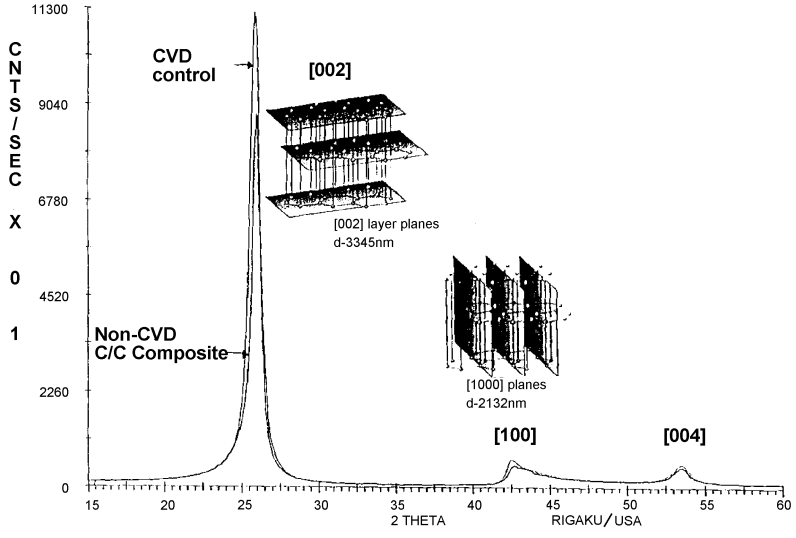

FIGURE 6 Carbon structure by wide-angle X-ray diffraction.

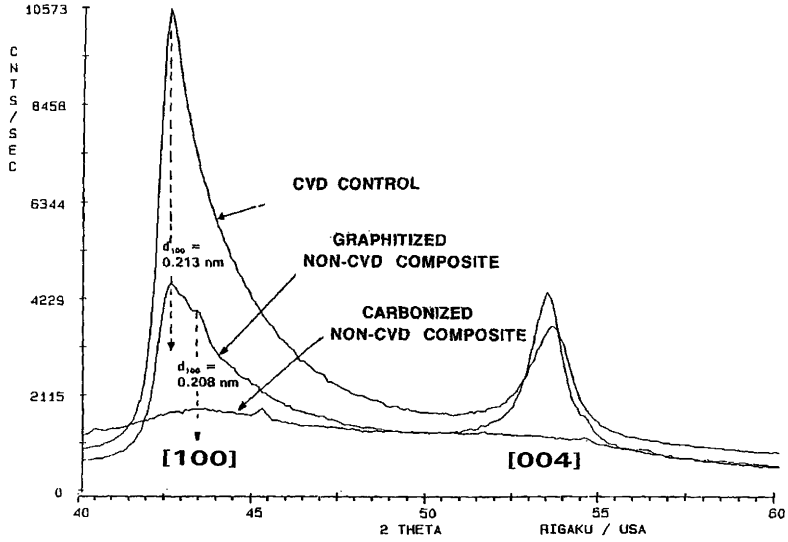

FIGURE 7 $d_{(100)}$ spacing by wide-angle X-ray diffraction.

TABLE 5 Effect of time

Spacing, nm		*Graphite crystal*	*Commercial CVD product*	*Non-CVD C/C composite* 0.5 *hr*	2.0 *hrs*	4.0 *hrs*
	$d_{(002)}$	0.335	0.342	0.344	0.345	0.344
1. $d_{(hkl)}$	$d_{(100)}$	0.213	0.212	(no reading)	0.212	0.212
2. $L_{c,(002)}$		Large	11.8	9.0	10.8	14.0
3. $L_{a,(100)}$		Large	6.3	(no reading)	4.8	4.6

TABLE 6 Effect of temperature

Spacing, nm		*Graphite crystal*	*Commercial CVD product*	*Non-CVD C/C composite* $< 1000°C$*	$1850°C$	$2000°C$
	$d_{(002)}$	0.335	0.342	–	0.345	0.343
1. $d_{(hkl)}$	$d_{(100)}$	0.213	0.212	0.208	0.212	0.212
2. $L_{c,(002)}$		Large	11.8	1.8	10.3	13.0
3. $L_{a,(100)}$		Large	6.3	2.1	4.6	5.6

*Carbonized composite.

RS – A 80. All the samples were fabricated at 1850°C and 5.0 kpsi by hot isostatic press for two hours. As indicated from Table 6, the dimensions of carbon structure grow with temperature. The structure grown at 2000°C is very similar to that found in the commercial product.

Compressive Strength of the One-Step Non-CVD C/C Composites

The compressive strength of the samples is measured when the sample is compressed to rupture (failure mode) between two parallel platens. The samples measured must have "identical" geometrical configurations. All of these samples evaluated, have otherwise, identical geometry of 0.75″ diameter × 0.4″ height.

Compressive strength for C – C composites of the same resin/fiber ratio is highly dependent on the density, or porosity. As seen in Figure 8 the higher the density, the better the compressive strength for the single step, non-CVD samples. Also, it shows that CVD samples have a density of approximately 1.77 gm/cc with compressive strength of about 27,000 psi. For the single step samples with the density of about 1.7 gm/cc, the compressive strength is about 33,000 psi. As the density drops to 1.5 gm/cc, the compressive strength decreases rapidly to about 15,000 psi. None of the samples that we tested, exhibited a buckling failure.

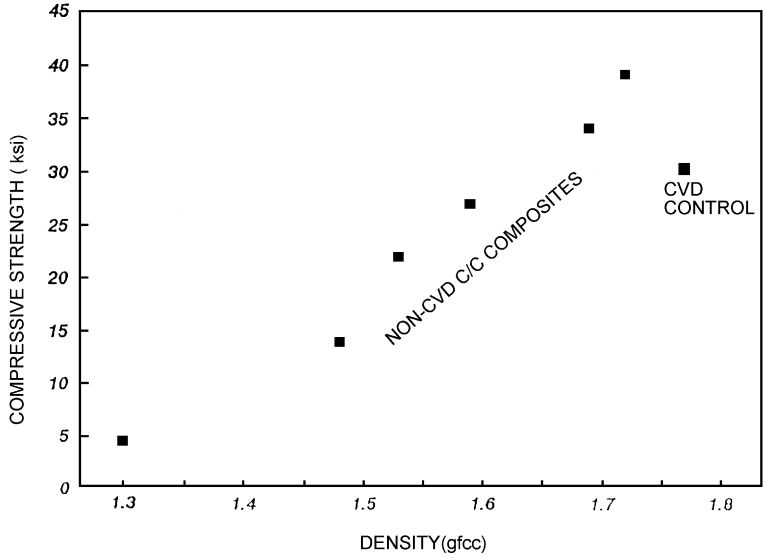

FIGURE 8 Density *vs.* compressive strength.

Conclusion

The results in Figure 8 show that our non-CVD process can lead to products having density exceeding 1.7 gm/CC which is somewhat below that values of commercial samples whose density is approximately 1.77 gm/cc. Despite this small difference in density, the non-CVD samples matched or exceeded the compressive strength of the commericial CC composites.

Friction and Wear Testing of Non-CVD C–C Composites: Effect of Graphitic Matrix Orientation

In our thrust to develop a one step non-CVD process for high performance C–C composites we encountered at this stage of research a major problem in an unexpectadly poor friction and wear characteristics of our Non-CVD composites.

We evaluated the wear resistance of six samples of Non CVD composites. Although the density and compressive strength of these composites was comparable to the commercial aircraft break control, their wear resistance was far below those of the commercial products. The results in Table 7, where the wear resistance is expressed in cycles to failure show than with respect wear, the non-CVD samples were more than an order of magnitude inferior to present commercial products.

To identify the causes of poor wear resistance of non-CVD composites we carried out the following sample characterizations:

1. Oxidative stability
2. Micro-cracking,
3. Fiber matrix interface,
4. Fiber breakage
5. Characteristics of the graphitic structure and
6. Graphitic matrix orientation

With respect to items 1–4 the comparative analyses produced no significant differences beween our non-CVD samples and the commercial CVD controls.

TABLE 7 Comparative properties of non-CVD C/C composite and CVD control

Sample	*Density g/cc*	*Compressive strength psi*	*Wear resistance*
			Cycles to failure
Single Step	1.66	22,000	20
ALS Control	1.77	27,000	256–357

In regard to graphitic matrix structure and oriention, however, the results revealed some important differences, that provided guidelines for the solution of the friction wear problem.

The X-ray data in Figure 9 showing the theta 2 theta scans from the CVD control and our non-CVD sample indicate that in addition to the differences in the orientation between the two samples discussed below there is also a significant difference in the structure of the carbon matrix. The $d(002)$ spacing of the CVD control is found to be 3.43 Å which indicates a predominantly amorphous glassy carbon structure. The non-CVD sample on the other hand exhibits two peaks one corresponding to the glassy carbon with the $d(002)$ spacing of 3.44 Å and a graphitic component with the $d(002)$ spacing of 3.37 Å. Since the graphitic structures are more stable at elevated temperatures and may have better mechanical properties than glassy carbon, we considered the presence of a graphitic phase in our samples advantageous.

With regard to matrix orientation, the X-ray data in Figure 9 show that the non-CVD sample exhibited a much higher level of the planar orientation of the (002) planes of graphite than the CVD control. Note that the (002) plane is the weak slip plane of graphite. Therefore, the planar orientation of these planes parallel to the friction surface should decreases the shear strength of the non-CVD samples parallel to the friction surface. Since this direction is parallel to the direction of shear stresses that exist in the

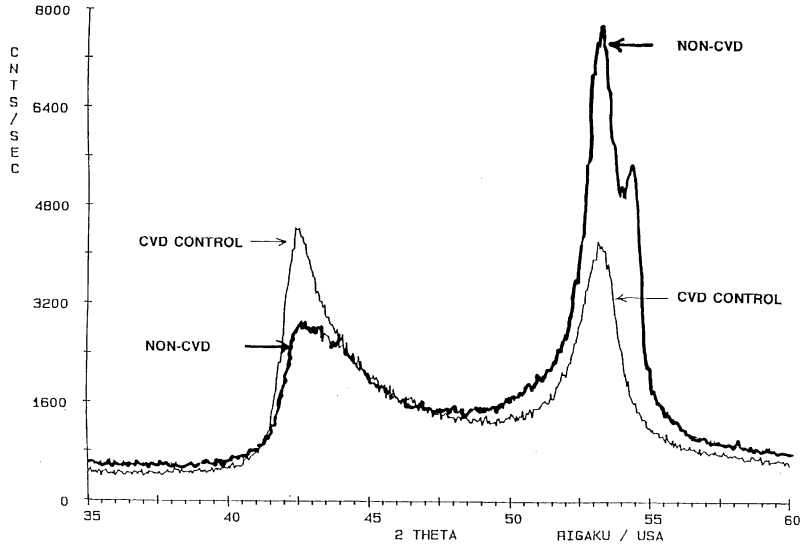

FIGURE 9 2 Theta scans from CVD control and non-CVD composites.

composite during friction experiments, we concluded that that the poor wear resistance of our non-CVD composites should be attributed to the high level of (002) plane orientation parallel to the friction surface.

To verify the postulated correlation between the matrix orientation and friction wear, we carried out with our non-CVD samples experiments in which the friction surface was oriented perpendicular to the orientation of the matrix (002) planes. The experimental set up to conduct these experiment is schematically presented in Figure 10. As anticipated, the samples B with (002) planes perpendicular to the friction surface exhibited a 20 times higher wear resistance then the control in which the (002) planes were predominantly parallel to the friction surface (Tab. 8).

Based on these data we concluded that the matrix orientation is a major factor in wear resistance. The experimental set up to prove this finding

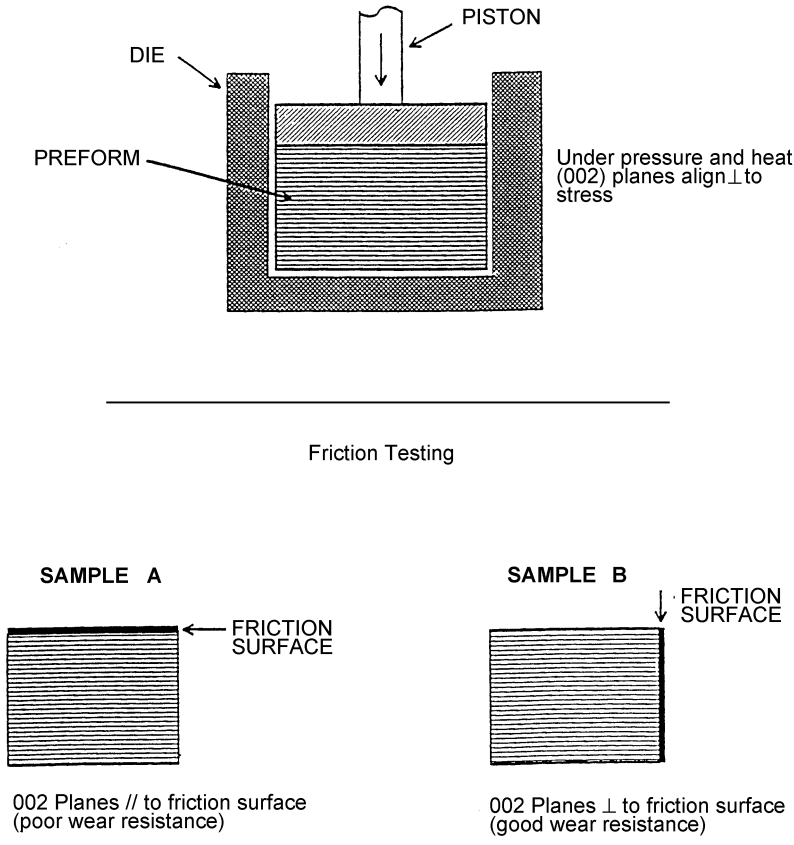

FIGURE 10 Non-CVD composites schematics of carbonization and graphitization control of (002) plane orientation.

TABLE 8 Effect of matrix orientation on wear resistance of non-CVD samples

Weight loss in 10 *minutes*		
Friction surface perpendicular to matrix orientation	*Friction surface parallel to matrix orientation*	(*Wt. loss parallel orientation*)/ (*Wt. loss prependicular orientation*)
118 mg	2221 mg	19
112 mg	3546 mg	32

On wear testing at CTC and ALS.

(Fig. 10) was, however, totally impractical for a commercially feasible process. The final phase of this program involved, therefore, development of an economical non-CVD process leading to products with acceptable (002) plane orientation and having properties meeting other mechanical and thermal requirements.

ONE STEP *Vs.* TWO STEP IMPREGNATION PROCESS

The last phase of this research involved the search for process modifications that will alter the morphology of the non-CVD samples into structures that are closer to those of present CVD products.

Critical experiment for this phase of our research is schematically presented in Figure 10. There is shown the process of sample preparation parallel and perpendicular to the applied stress during the carbonization step. Note that the wear resistance of the samples having the frictional surface parallel to the molding pressure had > 20 times smaller wear loss than the samples having the frictional surface perpendicular to the molding pressure.

After establishing the overriding role of morphology in the performance of these composites we needed to develop a working hypothesis regarding the optimal morphology. As previously with high performance Spectra fibers where we found useful correlations and feedback by studying the structure of these fibers and the structure of Nacre of see- shells. We aimed in the cases of non-CVD C – C composites to duplicate as much as possible the structure of the horse hoof. The hoof is made of keratin fibers found also in human nails, that, as we know, crack quite easily. But despite this obvious weakness, the problem of crack formation and propagation is solved in hoofs by the morphology shown schematically in Figure 11. Since the similarity between the stresses in horse hoof and those in aircraft and other friction materials during use is quite apparent, we were interested in finding how did the evolution solve these technological problem.

Three factors prompted our interest in hoof structure. First, we must recognize that the horse hoofs are like finger nails dead tissues and therefore, cannot heal themselves. Therefore, it is imperative that the structure of the

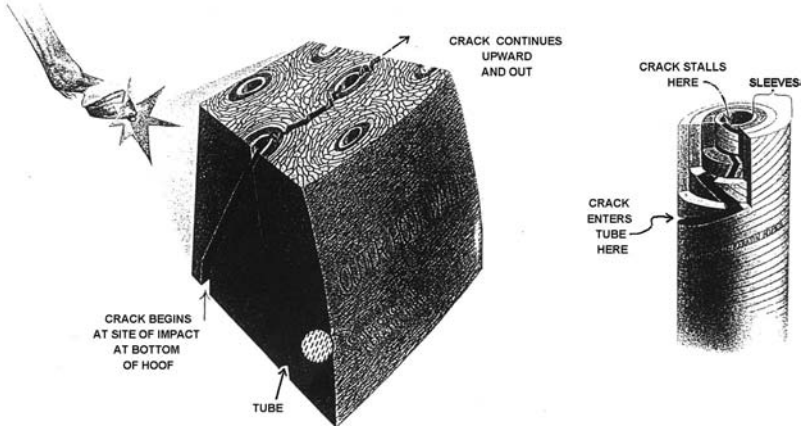

FIGURE 11 Schematics of structure and crack propagation of horse hoof (from Ref. [34]).

hoof withstand very large stresses without cracking. Second, these critical stress requirements have been achieved using relatively week materials that body can produce. Third, the final result is a result of the sophisticated composite structure and the horse hooves belong despite their relatively week components to the group of most crack-resistant materials. Their toughness is about twenty times higher than that of the bone.

The comparisons of the structure of horse hoofs presented schematically in Figure 11 and that of a non-CVD composite in Figure 12. (documented by SEM) prove that these materials have many common features. Therefore, it was understandable that we expected to obtain some useful information from the previous studies of horse hoof structure despite the fact that the vertical hollow tubes in the hoof are in C–C composites replaced by the strong

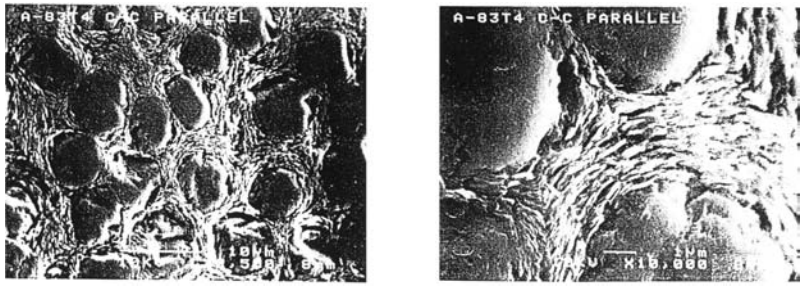

FIGURE 12 Matrix tile structure and its orientation in Non-CVD C–C composites.

carbon fibers. On the basis of these considerations we identified the following critical process parameters of a complete product optimization plan.

We concluded that such a plan should involve the following process variables: starting materials, pressure, strains and temperature profiles during carbonization, leading to optimal fiber and LC phase orientations in the final product.

The last factor, the optimal preform structure (3D weave characteristics) yielding after compressive carbonization strains the desired fiber orientations, eliminated the use of chopped impregnated fiber strands.

The braided keratin fiber structure with alternating right- and left-handed helices could possibly be achieved with reimpregnations. This, pointed to the advantages of a two or multiple impregnation process. Considering the complexity of the problem and the costs of a comprehensive optimization research we also recognized that at this stage of research we must carry out a relatively small number of experiments using the processing conditions selected on the basis the data available at that time.

For these experiments we chose a two step impregnation process involving the following steps:

Preform selection,
RTM impregnation,
Pyrolysis at ~1000°C at 0 stress,
Reimpregnation,
Heat treatment under pressure.

The results of 5 experiments of this series presented in Table 9 led to the following conclusions:

Density exceeding ~1.6 is required for a reasonable wear resistance.

Two step impregnation can reduce the compaction strain by as much 45%.

The optimal pressure for this process is at about ~7 ksi.

TABLE 9 Two step impregnation process. Effect of pressure on density, compaction and wear resistance

Sample	*Temp°C*	*Time/h*	*Pressure ksi*	*Density gm/cc*	*Comp. strain %*	*Wear-loss* $gm/s \times 10^{-4}$
CVD control				1.72		0.2
NON-CVD-1	1400	4	10.1	1.62	21	0.125
NON-CVD-2	1400	4	7.0	1.63	17	0.07
NON-CVD-3	1400	4	3.0	1.48	7	8.60
NON-CVD-4	1400	4	3.0	1.48	7	–
NON-CVD-5	1400	4	0.58	1.35	3	337.00

The sample having compaction strain of 21% performs with respect to wear poorer than a lower density sample having compaction strain of 17%.

The wear of a 10 KSI, 1.68 density and 21% compaction strain sample was almost twice as high as that of the sample prepared at 7 KSI pressure that had a density of 1.63 and compaction strain of 17%.

Most importantly, with a 28 hour non-CVD process described in this study we obtained samples that were on the laboratory scale 3-times more wear resistant than the samples currently produced in about 1000 hours using the standard CVD process.

CONCLUSIONS

A two step non-CVD process described in this study leads to satisfactory products in process times that are about 30 times shorter than those of standard CVD process. This reduction in process times is achieved by carrying the pyrolysis to maximal possible levels outside the carbon fiber preform.

The limits of pyrolysis are established by the rheological characteristics of the intermediated prestaged product allowing a satisfactory impregnation of the carbon fiber preforms.

In addition, this study also produced guidelines for future research aimed at product optimizations and tailoring of products for new applications. In this respect, the mimicking of the horse-hoof structure appears to be particularly promising.

In regard to matrix morphology, the most important finding was the importance of the (002) plane orientation, a factor neglected in all previously reported studies.

REFERENCES

[1] Prevorsek, D. C. and Sharma, R. K. (2002). *Int. J. Polym. Mater.*, **51**, 429.
[2] White, J. L. and Price, R. J. (1974). *Carbon*, **12**, 321.
[3] White, J. L. and Shaeffer, P. M. (1989). *Carbon*, **27**, 697.
[4] Marsh, H. and Walker, P. L. Jr. (1979). In "*Chemistry and Physics of Carbon*", Walker, P. L. and Thrower, P. A. Ed., **15**, 229.
[5] Collett, G. W. and Rand, B., "Rheological Investigation of Coal-tar Pitch during its Transformation to Mesophase", *Fuel*, **57**, 162, March, 1978.
[6] Wiecek, I., "*Rheological Properties of Mesophase Pitches from Coal Tar Pitch*".
[7] Bhatia, G., Aggarwal, R. K., Chari, S. S. and Jain, G. C. (1977). "Rheological Characteristics of Coal Tar and Petroleum Pitches with and without Additives", *Carbon*, **15**, 219.
[8] Balduhm, R. and Fitzer, E. (1980). "Rheological properties of Pitches and Bitmina up to Temperatures of 500°C", *Carbon*, **18**, 155.
[9] Nazem, F. F., "Rheology of Carbonaceous Mesophase Pitch", *Fuel*, **59**, 851, December, 1980.

[10] Fitzer, E., Kompalik, D. and Yudate, K., "Rheological Characteristics of Coal-tar Pitches", *Fuel*, **66**, November, 1987.
[11] Rand, B., "Carbon Fibers From Mesophase Pitch", In: "Strong Fibers" (Watt, W. and Perov, B. V. Eds.), pp. 495–575, North-Holland-Amsterdam, New York, 1985.
[12] Donnet, J.-B., "*Carbon Fibers*", Second Edition, Marcel Dekker, Inc., New York, 1990.
[13] Harry, H. and Walker, P. L. Jr., "The Formation of Graphitzable Carbons *Via* Mesophase: Chemicial and Kinetic Consideration", In: Walker, P. L. Jr. and Thrower, P. A., "*Chemistry and Physics of Carbon*", **15**, 229–286, Marcel Dekker, New York, 1979.
[14] Lafdi, F., Bonnamy, S. and Oberlin, A. (1991). *Carbon*, **29**(7), 831–864.
[15] Johnson, W., "The Structure of PAN Based Carbon Fibers and Relationship to Physical Properties", In: "*Strong Fibers*" (Watt, W. and Perov, B. V. Eds.), pp. 389–473, North-Holland-Amsterdam, New York, 1985.
[16] Fitz Gerald, J. D., Pennock, G. M. and Taylor, G. H. (1991). *Carbon*, **29**(2), 139–164.
[17] Kowbel, W. and Don, J. (1989). *J. Mater. Sci.*, **24**, 133–138.
[18] Shioya, M. and Takaku, A. (1990). *Carbon*, **28**(1), 165–168.
[19] Maire, J. and Mering, J., "Graphitization of Soft Carbons", In: "*Chemistry and Physics of Carbon*" (Walker, P. L. Jr. Ed.), **6**, 125–190, Marcell Dekker, New York, 1970.
[20] Weisshaus, H., Kenig, S., Kastner, E. and Siegmann, A. (1990). *Carbon*, **28**(1), 125–135.
[21] Chlopek, J. and Blzewicz, S. (1991). *Carbon*, **29**(2), 127–131.
[22] Moet, A. and Aglan, H., "Carbon–Carbon Composites", In: "*High Performance Polymers*" (Baer, E. and Moet, A. Eds.), pp. 135–172, Hanser Publishers, New York, 1991.
[23] Kowbel, W. and Shan, C. H. (1990). *Carbon*, **28**(2/3), 287–299.
[24] Lahaye, J., Louys, F. and Ehrburger, P. (1990). *Carbon*, **28**(1), 137–141.
[25] Rellick, G. (1990). *Carbon*, **28**(4), 589–594.
[26] Manocha, L. M., Bahl, O. P. and Singh, Y. K. (1991). *Carbon*, **29**(3), 351–360.
[27] Weisshaus, H., Kenig, S., Kastner, E. and Siegmann, A. (1991). *Carbon*, **29**(8), 1203–1220.
[28] Economy, J., Jung, H. and Gogeva, T. (1992). *Carbon*, **30**(1), 81–85.
[29] Manocha, L. M., Yasuda, E., Tanabe, Y. and Kimura, S. (1988). *Carbon*, **26**(3), 333–337.
[30] Meetham, G. W. (1991). *J. Mater. Sci.*, **26**, 853–860.
[31] Zaldvar, R. J. and Rellick, G. S. (1991). *Carbon*, **29**(8), 1155–1163.
[32] Noda, T. (1968). *Carbon*, **6**, 125–133.
[33] Franklin, R. E. (1951). *Proc. R. Soc.* (*London*), Ser. A, **A209**, 196.
[34] Zimmer, C. (1999). *Natural History*, **108**(9), 30.